NRC·CNRC

NRC Publications Archive
Archives des publications du CNRC

Lactone-bound structures of cyclohexanone monooxygenase provide insight into the stereochemistry of catalysis

Yachnin, Brahm J.; McEvoy, Michelle B.; Maccuish, Roderick J. D.; Morley, Krista L.; Lau, Peter C. K.; Berghuis, Albert M.

This publication could be one of several versions: author's original, accepted manuscript or the publisher's version. / La version de cette publication peut être l'une des suivantes : la version prépublication de l'auteur, la version acceptée du manuscrit ou la version de l'éditeur.
For the publisher's version, please access the DOI link below./ Pour consulter la version de l'éditeur, utilisez le lien DOI ci-dessous.

Publisher's version / Version de l'éditeur:
https://doi.org/10.1021/cb500442e
ACS Chemical Biology, 9, 12, pp. 2843-2851, 2014-09-29

NRC Publications Record / Notice d'Archives des publications de CNRC:
https://nrc-publications.canada.ca/eng/view/object/?id=1e2b203d-281c-480e-8f7c-309ea82bfa26
https://publications-cnrc.canada.ca/fra/voir/objet/?id=1e2b203d-281c-480e-8f7c-309ea82bfa26

Access and use of this website and the material on it are subject to the Terms and Conditions set forth at https://nrc-publications.canada.ca/eng/copyright
READ THESE TERMS AND CONDITIONS CAREFULLY BEFORE USING THIS WEBSITE.

L'accès à ce site Web et l'utilisation de son contenu sont assujettis aux conditions présentées dans le site https://publications-cnrc.canada.ca/fra/droits
LISEZ CES CONDITIONS ATTENTIVEMENT AVANT D'UTILISER CE SITE WEB.

Questions? Contact the NRC Publications Archive team at PublicationsArchive-ArchivesPublications@nrc-cnrc.gc.ca. If you wish to email the authors directly, please see the first page of the publication for their contact information.

Vous avez des questions? Nous pouvons vous aider. Pour communiquer directement avec un auteur, consultez la première page de la revue dans laquelle son article a été publié afin de trouver ses coordonnées. Si vous n'arrivez pas à les repérer, communiquez avec nous à PublicationsArchive-ArchivesPublications@nrc-cnrc.gc.ca.

National Research Council Canada | Conseil national de recherches Canada

Canada

ACS chemical biology

Articles

pubs.acs.org/acschemicalbiology

Lactone-Bound Structures of Cyclohexanone Monooxygenase Provide Insight into the Stereochemistry of Catalysis

Brahm J. Yachnin,[†,⊥] Michelle B. McEvoy,[†,⊥] Roderick J. D. MacCuish,[†] Krista L. Morley,[∥] Peter C. K. Lau,[§,#] and Albert M. Berghuis*[,†,‡,⊥]

Departments of [†]Biochemistry and [‡]Microbiology & Immunology, McGill University, 3649 Promenade Sir William Osler, Bellini Pavilion, Room 466, Montreal, Quebec, Canada H3G 0B1

[§]Departments of Microbiology & Immunology and Chemistry, McGill University, 3775 University Street, Montreal, Quebec, Canada H3A 2B4

[∥]National Research Council of Canada, 6100 Royalmount Avenue, Montreal, Quebec, Canada H4P 2R2

[⊥]Groupes de recherche GRASP et PROTEO, Montreal, Quebec, Canada

[#]FQRNT Center for Green Chemistry and Catalysis, Montreal, Quebec, Canada

Supporting Information

ABSTRACT: The Baeyer–Villiger monooxygenases (BVMOs) are microbial enzymes that catalyze the synthetically useful Baeyer–Villiger oxidation reaction. The available BVMO crystal structures all lack a substrate or product bound in a position that would determine the substrate specificity and stereospecificity of the enzyme. Here, we report two crystal structures of cyclohexanone monooxygenase (CHMO) with its product, ε-caprolactone, bound: the $CHMO_{Tight}$ and $CHMO_{Loose}$ structures. The $CHMO_{Tight}$ structure represents the enzyme state in which substrate acceptance and stereospecificity is determined, providing a foundation for engineering BVMOs with altered substrate spectra and/or stereospecificity. The $CHMO_{Loose}$ structure is the first structure where the product is solvent accessible. This structure represents the enzyme state upon binding and release of the substrate and product. In addition, the role of the invariant Arg329 in chaperoning the substrate/product during the catalytic cycle is highlighted. Overall, these data provide a structural framework for the engineering of BVMOs with altered substrate spectra and/or stereospecificity.

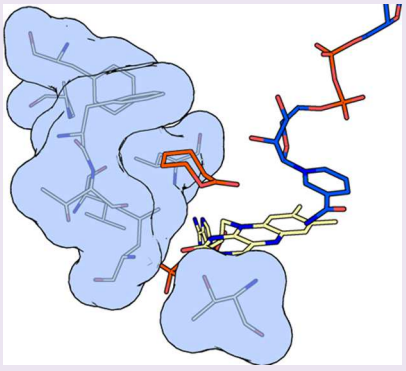

For over 100 years, the Baeyer–Villiger oxidation (BVO) reaction has been used for the synthesis of esters and lactones from ketones.[1,2] A wide range of synthetic applications, including in the production of polymers, perfumes, drugs, and other bioactive molecules, have been developed.[3] The "classical" oxidative reagents in BVO, however, are peracids, with the original BVO reaction being performed with Caro's acid. These reagents are hazardous, especially on an industrial scale, and require the extensive use of organic solvents. The reaction can also lack the stereospecificity required for synthesis of pharmaceutical compounds, necessitating the use of additional cleanup steps. This has led to attempts to develop alternative reagents, such as transition metal catalysts,[4,5] for BVO reactions. These catalysts unfortunately tend to be expensive, and the reaction in general must still be performed in organic solvents.

An alternative to conventional chemical catalysts are the Baeyer–Villiger monooxygenases (BVMOs), a group of enzymes, primarily of bacterial origin, that can catalyze the BVO reaction. These enzymes have been extensively studied since the 1970s.[6,7] The BVMOs are FAD-dependent enzymes that are notable for exhibiting high stereospecificity in many cases, while still having a broad substrate spectrum, making them quite versatile.[8−13] They only require NADPH and oxygen as cosubstrates for the reaction and produce only $NADP^+$ and water as byproducts. Genome mining has led to the identification of a number of BVMOs in recent years, increasing the spectrum of substrates that can be targeted by BVMOs.[13]

As with any potential biocatalyst, it is important to be able to redesign the biocatalyst for specific industrial applications. While a number of directed evolution studies have led to improved or redesigned BVMOs,[14−21] a complete understanding of the structural mechanism of BVMOs is necessary to perform rational protein design. The first step toward this goal came a decade ago, with the publication of the first crystal structure of a BVMO, phenylacetone monooxygenase (PAMO), in complex with FAD.[22] This was followed by two distinct crystal structures of cyclohexanone monooxygenase (CHMO) from *Rhodococcus* sp. HI-31 (*Rm*CHMO) in complex with FAD and $NADP^+$, known as the $CHMO_{Open}$ and $CHMO_{Closed}$ crystal structures.[23] These two structures high-

Received: June 3, 2014
Accepted: September 29, 2014
Published: September 29, 2014

 © 2014 American Chemical Society dx.doi.org/10.1021/cb500442e | *ACS Chem. Biol.* 2014, 9, 2843−2851

lighted the dynamic properties of the enzyme, characterized by domain rotations and the order/disorder transition of a large loop.[23]

Following the publication of these three structures, reports of several more PAMO structures, in complex with $NADP^+$ as well as a weak inhibitor, were solved.[24] The PAMO structures allowed the comparison of the oxidized and reduced states of FAD. In addition, a series of structures of 2-oxo-Δ^3-4,5,5-trimethylcyclopentenylacetyl-coenzyme A monooxygenase (OTEMO)[25] were solved, representing the first BVMO crystal structures of a dimeric BVMO, and also of a BVMO that acts on a very large substrate. A distantly related BVMO, MtmOIV, has also been solved both in the presence[26] and in the absence[27] of its substrate, premithramycin B. MtmOIV is more closely related, by sequence and structure, to the hydroxylases PgaE and CabE than to the classical BVMOs.

The first crystal structure of a classical BVMO with a known substrate or product bound was that of CHMO bound to cyclohexanone, known as the $CHMO_{Rotated}$ structure.[28] In this crystal structure, the $NADP^+$ cofactor was rotated away from the flavin ring system, allowing the substrate to take its place. This places the substrate in position for the formation of the Criegee intermediate without imposing steric constraints on the substrate, thereby rationalizing the broad substrate specificity[23] of the enzyme.

While the broad substrate specificity of CHMO could be rationalized based on the $CHMO_{Rotated}$ structure, the stereospecificity and substrate profile could not. The large size of the cavity where the substrate sits makes it difficult to explain substrate selection or stereospecificity. In addition, a number of residues that have been implicated, through mutagenesis and directed evolution studies, in the determination of the substrate profile and stereospecificity of the enzyme[14−21] are distant from the substrate in the $CHMO_{Rotated}$ structure. It was suggested that the substrate should bind in the pocket previously predicted based on the $CHMO_{Closed}$ structure for the determination of substrate acceptance and stereospecificity. The enzyme would then switch to the Rotated conformation to allow the formation of the Criegee intermediate.[28]

Here, we present the first two crystal structures of any BVMO with its product, ε-caprolactone, bound. To differentiate these structures, we refer to them as the $CHMO_{Tight}$ and $CHMO_{Loose}$ structures. These two structures can be seen as being analogous to the previously reported $CHMO_{Closed}$ and $CHMO_{Open}$ structures, respectively. In both crystal structures, the lactone sits in roughly the position that would have been predicted based on the $CHMO_{Closed}$ structure,[23] making them the first crystal structures with a natural ligand at this position. This places the product in close proximity to those residues implicated in substrate specificity and stereospecificity[14−21] and allows us to propose a structural framework for the basis of the stereospecificity of the enzyme. While this kind of structural framework has been the goal of several recent computational studies,[29−31] it is clear that the experimental data presented here will greatly facilitate these efforts. Furthermore, the differences between the two structures allow us to present a three state binding mechanism that is consistent with and extends the previously proposed structural mechanism (Figure S1).[28]

RESULTS AND DISCUSSION

Results. *Crystal Structures of CHMO in Complex with Its Product.* The $CHMO_{Tight}$ and $CHMO_{Loose}$ structures were solved to 1.94 and 2.5 Å, respectively. Of the 540 residues in the *Rm*CHMO sequence (excluding the remainder of the cleaved N-terminal His-tag), the $CHMO_{Tight}$ structure could be modeled from residues 6−534, whereas the $CHMO_{Loose}$ structure could be modeled from residues 6−533. As previously observed in the $CHMO_{Open}$[23] and $CHMO_{Rotated}$[28] structures, a large loop ranging from residues 489−505 was not visible in the $CHMO_{Loose}$ electron density map and was therefore omitted from the model. Both the $CHMO_{Tight}$ and $CHMO_{Loose}$ structures had clearly defined density for both the FAD and $NADP^+$ cofactors. Of note, in spite of the disordering of the loop in the $CHMO_{Loose}$ structure, both structures had the $NADP^+$ molecule in a similar conformation, as was previously observed in the $CHMO_{Closed}$ structure.[23] This makes the $CHMO_{Loose}$ structure the first structure with the loop disordered, but with $NADP^+$ in the Closed-like, "pushed in" position. The $CHMO_{Loose}$ crystal structure, which was cross-linked using glutaraldehyde, had density visible beyond the end of Lys40 and also connecting Lys174 to Arg179. The former was modeled as a glutaraldehyde modification to Lys40, whereas the latter was modeled as a glutaraldehyde bridge between Lys174 and Arg179 as described by Salem et al.[32] It should be noted that these modifications do not substantially perturb the configuration of these residues compared to other CHMO crystal structures.

In spite of the fact that both of these structures have the same set of ligands bound, these structures are not identical. Indeed, the $CHMO_{Tight}$ structure more closely resembles the $CHMO_{Closed}$ structure, with an RMSD of 0.42 Å for backbone atoms present in both structures after overlaying the FAD-binding domains. This compares to an RMSD of 0.61 Å when comparing the $CHMO_{Loose}$ and $CHMO_{Tight}$ structures. The $CHMO_{Loose}$ structure resembles the $CHMO_{Rotated}$ structure marginally more than it resembles $CHMO_{Tight}$, with an RMSD of 0.59 Å. These variations once again highlight the importance of BVMO protein dynamics first proposed based on the original PAMO structure[22] and confirmed based on the three previous CHMO structures.[23,28]

That cross-linking allows us to capture a state in which the NADPH-binding domain is rotated and the large loop is disordered compared to the $CHMO_{Tight}$ structure, rather than stabilizing the $CHMO_{Tight}$ structure as expected, was quite surprising. In order for glutaraldehyde to alter the conformation of crystals, the $CHMO_{Tight}$ crystals must exist in an equilibrium between the Tight-like and Loose-like conformations, at least at room temperature. The cooling of the $CHMO_{Tight}$ crystals to cryogenic temperatures prior to data collection may be responsible for locking the rotational position of the NADPH-binding domain in the crystal, as well as the ordered conformation of the loop. The cross-linking of the crystals is likely responsible for stabilizing the alternative conformation observed in the $CHMO_{Loose}$ crystal structure.

When the two new CHMO structures are overlaid onto the three available CHMO structures, using the FAD-binding domains to superimpose them, the degree of rotation of the NADPH-binding domain in each structure becomes evident. The two extremes of domain rotation remain the $CHMO_{Open}$ and $CHMO_{Closed}$ structures. For the three structures that have a ketone substrate or lactone product bound, the $CHMO_{Rotated}$ structure is closest to the $CHMO_{Open}$ structure, while the $CHMO_{Tight}$ structure is closest to the $CHMO_{Closed}$ structure. This means that starting with the $CHMO_{Open}$ structure, a gradual closing of the NADPH-binding domain can occur by

dx.doi.org/10.1021/cb500442e | ACS Chem. Biol. 2014, 9, 2843−2851

transitioning from structure to structure in the following order: $CHMO_{Open} \rightarrow CHMO_{Rotated} \rightarrow CHMO_{Loose} \rightarrow CHMO_{Tight} \rightarrow CHMO_{Closed}$ (Figure S2).

ε-Caprolactone Is in the Substrate Binding Site: $CHMO_{Tight}$ Crystal Structure. Upon initial solution of the $CHMO_{Tight}$ crystal structure, a number of characteristics of the structure suggested that it was distinct from others obtained under similar conditions, but in the absence of ε-caprolactone. The most obvious of these was the ordering of the loop from residues 487−505, which was consistently disordered in the absence of either ketone or lactone, and also in the presence of cyclohexanone. In addition, the conformation of $NADP^+$, which resembled either the $CHMO_{Open}$ or $CHMO_{Rotated}$ structure in the absence of the lactone, adopted the conformation observed in the $CHMO_{Closed}$ structure. Finally, crystals obtained in the absence of either substrate or product would lack the orthorhombic symmetry and yield a monoclinic crystal with unit cell angles all equal to 90° and with two protein molecules in the asymmetric unit.

Close examination of the electron density map in the area identified in the $CHMO_{Closed}$ structure as a putative substrate binding pocket[23] revealed a ring-shaped region of electron density corresponding to the size and shape of ε-caprolactone. Upon modeling the lactone in this site, this ring of density remained visible in the weighted $2F_o-F_c$ map, but only when the map was contoured at 0.6 sigma (Figure 1a). At 1.0 sigma, density corresponding to the carbonyl group and the ring oxygen was visible, while density for the remaining carbons was very weak or not visible at all. This suggested that while the product may be present in this crystal structure, it was unlikely to be present at full occupancy. On the basis of the contour level of the weighted $2F_o-F_c$ electron density map at which the full lactone ring was visible, the occupancy for the lactone was set to 0.6.

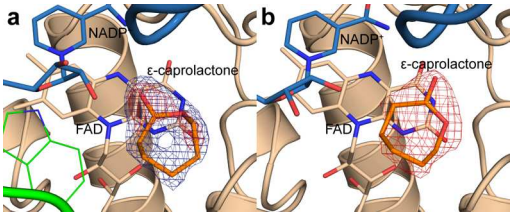

Figure 1. Electron density map for ε-caprolactone in the (a) $CHMO_{Tight}$ and (b) $CHMO_{Loose}$ crystal structures. The $2F_o-F_c$ map is shown contoured at 0.6 sigma (blue, panel a only) and 1.0 sigma (red).

ε-Caprolactone Is in the Substrate Binding Site: $CHMO_{Loose}$ Crystal Structure. In order to corroborate the presence of the lactone in the $CHMO_{Tight}$ structure, it was decided to cross-link the crystals with glutaraldehyde and soak in more ligand than could normally be tolerated by the crystals. It was expected that this would lead to a very similar structure with better defined density for the lactone. Surprisingly, there were a number of alterations in the crystal structure that suggested a more dynamic conformation than the original, non-cross-linked crystals, as previously discussed. Note that since these changes require alterations within an already formed crystal, it is likely that the lower resolution and slightly elevated R-factors of the $CHMO_{Loose}$ structure are due to perturbations in the crystal lattice caused by the cross-linking reaction.

One characteristic of this structure was the disordering of the large loop spanning residues 489−505, resulting in a much more open active site. It is likely for this reason that the soaking experiments appear to have been so successful. There was clearer density in the same location in which the ligand was observed in the $CHMO_{Tight}$ structure. When ε-caprolactone was modeled in at this position, the weighted $2F_o-F_c$ map contoured at 1.0 sigma clearly shows a fairly strong region of electron density corresponding to the lactone (Figure 1b). This is in spite of the lower resolution of this crystal structure.

ε-Caprolactone Is in the Substrate Binding Site: Comparison of the Lactone Positions. As the two ε-caprolactone-bound crystal structures are not isomorphic, it became necessary to compare the binding mode of the lactone in the two structures. When the two structures are overlaid, the lactone is found to sit in almost exactly in the same place (Figure S3a). There is, however, a rotation of roughly 30° that causes a displacement of the position of the carbonyl oxygen. This shift could be related to the disordering of the large loop in the $CHMO_{Loose}$ structure. The lack of strong features in the electron density map of the $CHMO_{Loose}$ structure, however, means that unlike in the $CHMO_{Tight}$ structure, there is some ambiguity in the rotational position of the lactone in the $CHMO_{Loose}$ structure. This could reflect greater freedom of movement for the ligand in the Loose conformation.

When comparing all of the residues that are within 6.0 Å of either lactone in either structure, most of the residues sit in the same position in both structures. The RMSD for all atoms in these residues, excluding residues 145 and 146, which form part of the flexible linker loop between the FAD-binding and NADPH-binding domains, is 0.7 Å. This suggests that the residues critical for recognizing the lactone remain in the same position in spite of the conformational changes observed in the global protein conformation (Figure S3b).

Binding Site Properties of the Lactone-Bound Structures. While the residues in close proximity to the lactone remain in a similar position in both lactone-bound crystal structures, there remains a significant difference in the ligand binding site in these structures. The rotation of the NADPH-binding domain and concurrent order−disorder transition of the large loop spanning residues 489−505 results in a change in the solvent accessibility of the binding site. In the $CHMO_{Loose}$ crystal structure, the position of the NADPH-binding domain and the disorder of the large loop results in a fairly open binding site (Figure 2a), though not quite as large as what is observed in the $CHMO_{Open}$ crystal structure.[23] The $CHMO_{Tight}$ structure, in contrast, has a binding site that is roughly the same size as the small binding pocket observed in the $CHMO_{Closed}$ crystal structure[23] (Figure 2b). This appears to suggest that the lactone is being bound in two alternative binding modes, which

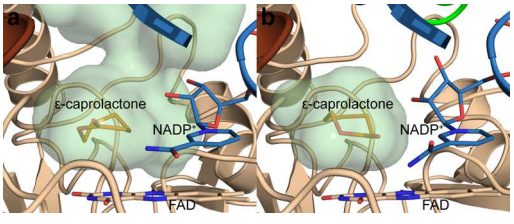

Figure 2. Comparison of the ε-caprolactone binding site in the (a) $CHMO_{Loose}$ and (b) $CHMO_{Tight}$ crystal structures. The available space for the ligand is shown as a transparent green surface.

dx.doi.org/10.1021/cb500442e | ACS Chem. Biol. 2014, 9, 2843−2851

provides the rationale for the naming of these two structures. The $CHMO_{Tight}$ structure reflects a tighter binding mode that is likely important for substrate selection and orientation. The $CHMO_{Loose}$ structure appears to reflect a looser binding mode which may reflect an initial association and final disassociation between the ligand and the enzyme. This structural state is likely more dynamic than the Tight conformation. The similarity to the $CHMO_{Open}$ structure, however, does suggest that the Loose conformation is a distinct structural state and not simply an artifact of the glutaraldehyde cross-linking.

Effects of the W492A on Substrate Profile. Residue Trp492, which is the only residue in the 487−504 loop within 3.5 Å $NADP^+$ in the $CHMO_{Closed}$ and the $CHMO_{Tight}$ structures, has previously been shown to be catalytically important, though not essential. The W492A mutant was shown to have substantially lower activity as well as decreased $NADP^+$ affinity.[23] In order to assess the impact of the loop ordering on the substrate profile of the enzyme, the substrate profile of the wild-type enzyme was compared to that of the W492A mutant. The isopropanol controls demonstrated that the mutant is prone to increased uncoupling of NADPH consumption from substrate conversion, as the mutant completely consumed the NADPH within 1 day in the absence of substrate, whereas the NADPH was stable in the presence of the wild-type enzyme for several days.

Of the substrates tested, the mutant was found to be more selective in all cases, and in some cases became almost completely unable to transform certain substrates (see Table S1). Both 2-methyl and 2-propylcyclohexanone show gains in their *E* values, becoming increasingly *S*-selective. For 2,6-dimethylcyclohexanone, of the three possible isomers (*cis*, *R*/*R*-*trans*, and *S*/*S*-*trans*), it appears that the *cis*-isomer and one of the *trans*-isomers are both converted efficiently by the wild-type enzyme. In the case of the mutant, the enzyme loses the ability to convert the *cis*-isomer, converting only the same *trans*-isomer in significant quantities. For (+)-dihydrocarvone, the wild-type is already highly selective for the *trans*-isomer and produces essentially no lactone from the *cis*-isomer. In the mutant, we see almost a complete loss of activity, with the conversion rate dropping from 51% to 2%.

Discussion. *$CHMO_{Tight}$ is Likely the Conformation Where Stereospecificity Is Determined.* A number of directed evolution and mutagenesis studies have identified residues that, when altered, trigger changes in the substrates that can be accommodated by the BVMOs, as well as perturbations in the stereospecificity of the enzymes. Close to the flavin ring system, these include T60, L145, L428, P430, F434, T435, L437, and F507,[14−21] with all residues indicated with *Rm*CHMO residue numbering. It has been previously noted that the $CHMO_{Rotated}$ structure, which is in an ideal position for formation of the Criegee intermediate, does not place cyclohexanone close to these residues.[28] In contrast, both $CHMO_{Tight}$ and $CHMO_{Loose}$ place ε-caprolactone in close proximity to these key residues (Figure 3). Assuming that the substrate, in the presence of the peroxyanion intermediate, would also bind in the same manner as the product in our structures, this strongly suggests that the acceptance of substrates, as well as the regio- and enantiospecificity of the enzyme, is determined in the Loose and/or Tight conformations.

The existence of two distinct lactone-bound structures is indicative of a multistep binding mechanism. The more open binding pocket in the $CHMO_{Loose}$ structure is likely to be the first, Loose-binding mode. In this state, the enzyme will undergo the initial interaction with a potential substrate and likewise will be the last state prior to product release. It would be expected that this step would be fairly nonspecific. It may also vary slightly depending on the substrate and dynamic protein motions, thereby acting as a representative of a "family" of structural states. Once the substrate is associated with the enzyme, a conformational change will occur, causing the enzyme to adopt a second binding mode in the Tight conformation. The small, closed off binding pocket in this conformation would not be able to form in the presence of a molecule that is not an appropriate substrate for the enzyme. Likewise, if the substrate were to be in the "wrong" orientation for the proper stereospecificity of the enzyme, the conformational change would either not occur or force the substrate into the correct orientation. Once properly in the Tight conformation, the enzyme could then transition into the Rotated conformation to form the third binding mode and allow the formation of the Criegee intermediate.[28]

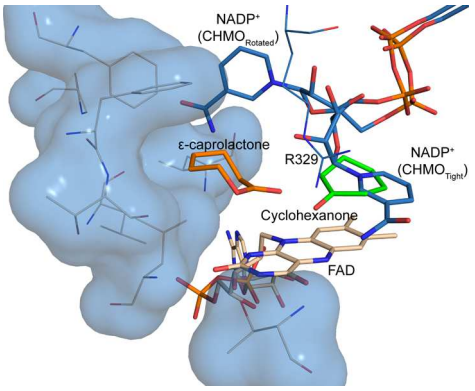

Figure 3. Position of ε-caprolactone relative to the residues important for substrate specificity in the $CHMO_{Tight}$ structure. Residues that have been shown to be important for substrate specificity are shown as a blue surface. Cyclohexanone from the $CHMO_{Rotated}$ structure (green) is shown for comparison.

The Stereospecificity of CHMO Can Be Predicted by the $CHMO_{Tight}$ Structure. One of the critical questions in developing a rational strategy for the re-engineering of BVMOs is the structural basis for the stereospecificity of the enzyme. To address this question, we need to identify which of the two carbons adjacent to the carbonyl will migrate to form the lactone product, once the substrate is bound in the Tight conformation. We will refer to this "decision" by the enzyme as the "directionality" of oxygen incorporation. The directionality can be seen as a single property that covers all ketone substrates. In contrast, chemical terms like "regiospecificity" and "enantiospecificity" will be determined by the directionality of the enzyme but will always depend on the stereochemical properties of the substrate and product in question.

Unfortunately, the resolution of the $CHMO_{Tight}$ and $CHMO_{Loose}$ structures is insufficient to differentiate between the oxygen and carbon atoms within the lactone ring, and thus we are unable to identify the directionality of oxygen incorporation exclusively from the diffraction data; however, it is possible to combine these data with stereospecificity data from CHMO and its mutants/homologues to determine the enzyme's directionality. Indeed, when considering five substrates across two BVMOs and one mutant, we can correctly predict which products would be produced if we assume that the BVMOs use consistent directionality based on the

dx.doi.org/10.1021/cb500442e | *ACS Chem. Biol.* 2014, 9, 2843−2851

$CHMO_{Tight}$ crystal structure. While we make the assumption that the directionality of oxygen incorporation will be the same for all substrates and all BVMOs, we must recognize that more data are required to confirm these assumptions as being generally true.

Our first example involves the F434S mutation of CHMO, which greatly improves the enzyme's enantiospecificity with respect to the prochiral substrate, 4-hydroxycyclohexanone.[14] When the energy-minimized substrate is placed in the wild-type lactone binding position, two possible configurations appear equally favorable (Figure 4a). In contrast, the mutated serine

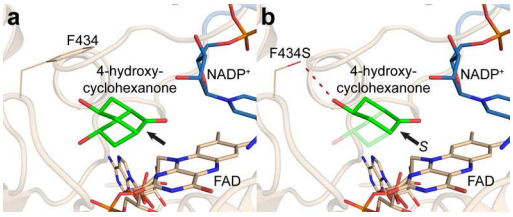

Figure 4. Enantiospecificity of CHMO for 4-hydroxycyclohexanone. (a) In the wild-type structure, neither the "up" nor the "down" configuration of the substrate is preferred. (b) In the F434S mutant, the "up" configuration is preferred due to the formation of a hydrogen bond. The positions of the substrate are modeled based on the position of ε-caprolactone in the $CHMO_{Tight}$ crystal structure. The directionality of the enzyme is indicated with the black arrow.

residue in F434S will form a hydrogen bond with only one of the two configurations, thereby favoring one configuration over the other (Figure 4b). This corresponds perfectly to the almost negligible enantiomeric excess (EE) of 9% in favor of the *R*-enantiomer in the wild-type, as compared to the large improvement in EE to 79% in favor of the *S*-enantiomer in the F434S mutant.[14] Based on the favored conformation in the $CHMO_{Tight}$ crystal structure and our prior knowledge that the *S*-enantiomer must be formed, we can determine which oxygen migrates to form the lactone, and by extension the directionality of the enzyme, as shown in Figure 4.

This stereochemical framework can be expanded by comparing the regiospecificity of terpenone substrates when converted by CHMO and cyclopentanone monooxygenase (CPMO; see Figure 5c).[33] Of the eight substrates reported in that manuscript, only the four substrates that were converted with reasonable reactivity and high regiospecificity were considered. There are four residues that differ between CHMO and CPMO that are in close enough proximity to the lactone binding site to have a direct effect on ligand binding: L145/F156, L428/Y442, L437/G453, and F507/N523 (residues are listed as *Rm*CHMO numbering/CPMO numbering). The carbonyl group of each substrate was overlaid onto the carbonyl group of ε-caprolactone in the $CHMO_{Tight}$ structure. As each substrate can be rotated 180° around the C═O bond, and the other half of the cyclohexanone ring (carbons 3−5) can be puckered either toward or away from the FAD molecule, each substrate has a total of four possible configurations in the Tight conformation. For more details, see the Supporting Methods.

The most likely of the four configurations for each of the energy-minimized substrates in the $CHMO_{Tight}$ structure was assessed first based on steric effects (see Figure 5 and Figure S4). We then considered whether the four CPMO substitutions would be likely to result in a change in the positioning of the

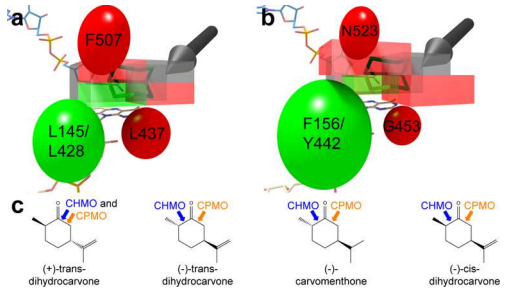

Figure 5. Regiospecificity of CHMO and CPMO for various terpenones (see also Figure S4). The three groups of residues that change between CHMO and CPMO are represented as ellipsoids, with residues that are more sterically demanding in CHMO represented in red and those that are more sterically demanding in CPMO represented in green. The substrate binding site is represented as a box, which is colored in red or green to correspond to the nearby ellipsoid. Those portions of the box that are not close to any ellipsoid are colored in gray. The two configurations of a cyclohexanone substrate are shown in green, and an arrow indicates the site of incorporation of the oxygen (see also Figure 4). (a) A representation of the CHMO binding site. (b) A representation of the CPMO binding site, with changes in the ellipsoid and box size emphasizing the changes in steric accessibility as compared to CHMO. (c) The regiospecificities of the four terpenones is shown, with the enzymes' preference for incorporating oxygen on the more substituted (chemically preferred, normal lactone product) or less substituted side (abnormal lactone product) of the carbonyl indicated with blue (CHMO) and orange (CPMO) arrows.

substrate. As seen in Figure 5, in those cases where the positioning was predicted to be switched, a change in the regiospecificity of the enzyme was observed. In addition, if the same directionality as observed in the 4-hydroxyclohexanone case is used for these four substrates, the correct lactone product is predicted in all eight cases.

We have used the $CHMO_{Tight}$ crystal structure to accurately predict the lactone products produced by two BVMOs and one mutant across five different substrates. In all cases, in order to obtain the correct stereochemistry for the products while accommodating the most likely energy-minimized substrate, the directionality of the enzyme must be the same. In the absence of independent experimental data, we feel that this provides compelling evidence for modeling the lactone as we have in the $CHMO_{Tight}$ and $CHMO_{Loose}$ crystal structures. As such, it provides the first framework for assessing substrate specificity and stereospecificity of the BVMOs based on a substrate- or product-bound crystal structure.

Transition from $CHMO_{Tight}$ to $CHMO_{Rotated}$. As previously described, it appears highly likely that substrate acceptance and directionality be determined in the Tight conformation, based on previous mutagenesis and directed evolution studies. Given that we expect the formation of the Criegee intermediate to occur in the Rotated conformation, we can hypothesize that the substrate should move from the Tight binding pocket to the Rotated binding pocket without giving the substrate the opportunity to reorient itself, as this reorientation would presumably cause the stereochemical requirements of the Tight binding pocket to be lost prior to the formation of the Criegee intermediate. While the enzyme could be using a number of different mechanisms to effect this repositioning, we believe that the most likely case is that the strictly conserved residue Arg329 plays a central role in maintaining the substrate's orientation through this conformational change (Figure 6). In

dx.doi.org/10.1021/cb500442e | *ACS Chem. Biol.* 2014, 9, 2843−2851

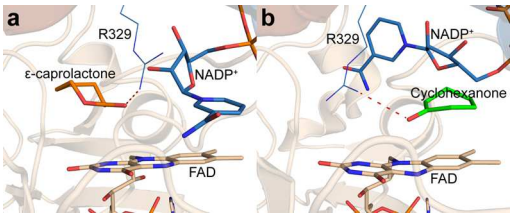

Figure 6. Arg329 may play a role in guiding the substrate and product from the Tight position to the Rotated position and back. The interaction between Arg329 and the carbonyl oxygen of cyclohexanone or ε-caprolactone is shown. (a) The $CHMO_{Tight}$ crystal structure. (b) The $CHMO_{Rotated}$ crystal structure.

the $CHMO_{Tight}$ structure, Arg329 forms a hydrogen bonding interaction with the carbonyl oxygen of ε-caprolactone. A strong interaction is formed with one of the terminal nitrogens, and a weaker interaction is formed with the ε-nitrogen. In the $CHMO_{Rotated}$ structure, Arg329 remains at a hydrogen bonding distance from the carbonyl oxygen of cyclohexanone. This suggests that Arg329 could play a role in guiding the substrate from the Tight position to the Rotated position without giving it the opportunity to reorient itself. Of course, it remains possible that the enzyme uses another (or an additional) mechanism to effect this transition.

With the enzyme adopting the Tight conformation, the question arises as to whether the Rotated conformation is still necessary. Indeed, the structure of PAMO bound to the inhibitor MES has previously been used to suggest that the Criegee intermediate would form with the substrate in a Tight-like pocket,[24] and computational studies have been used to model the reaction with cyclohexanone and its derivatives with small substituents forming the Criegee intermediate at that position.[30,31] The drawback of this interpretation is the inability to explain the larger substrates that can be accommodated.[23] Even if active site plasticity is invoked, which could be used to explain how a large, bicyclic substrate could bind in a Tight-like conformation, if the substrate were to get close enough to actually form the Criegee intermediate, it would clash with either $NADP^+$ or the residues on the opposite side of the lactone (Figure S5). For the former possibility, such a mechanism would require $NADP^+$ to slide deeper into the enzyme, for which there is no structural evidence and which appears unlikely based on the proximity of the protein surface to $NADP^+$ on that side. For the latter case, the residues on the opposite side of the lactone are in a relatively immobile region of the protein and therefore are unlikely to move. In contrast, if the Criegee intermediate is not required to form in a Tight-like conformation, the substrate could move out toward the opening seen in the $CHMO_{Open}$ and $CHMO_{Loose}$ structures without the constraint of being in close enough proximity to the FAD molecule to form the Criegee intermediate. The Tight-Rotated mechanism appears to be the only available explanation that is consistent with both the high stereospecificity and the ability to accommodate large substrates that is characteristic of CHMO.

The Role of the Loop in the Catalytic Cycle. As the large loop is disordered in the $CHMO_{Loose}$ structure and ordered in the $CHMO_{Tight}$ structure, it is easy to suggest that the ordering of the loop assists the enzyme in adopting the more selective, Tight conformation, thereby restricting the amount of space available to the substrate. It was therefore quite surprising to find that the W492A mutant, in which the key interaction between the loop and $NADP^+$ is eliminated, actually resulted in an enzyme that was more selective, if less active. These results are difficult to explain without further study of the dynamic properties of the loop and its effect on substrate profile. We can speculate that the loop acts as a "gatekeeper" to prevent the substrate from diffusing away from the active site. The W492A mutant may be decreasing the frequency of the "gate closing," allowing less preferred substrates or substrate conformations (i.e. substrates/conformations with a rapid k_{off} rate) to diffuse away more readily. Alternatively, it is also possible that that the W492A mutation, which reduces the hydrophobic character of the loop, would alter the loop's conformational behavior and, by extension, the nature of the substrate binding pocket.

Regardless of the actual mechanism for increasing the selectivity of the mutant, it is clear that this loop has a more complex role than previously thought, and that further study of this and other loop mutants in warranted. In particular, the increased selectivity of W492A suggests that this loop may be a useful target for further improvements in BVMO selectivity. While the diminished activity and increased uncoupling of the W492A mutant precludes its use as a good biocatalyst, it remains a possibility that other loop mutants, targeting either Trp492 or other loop residues, may be able to achieve this higher selectivity without sacrificing biocatalyst efficiency. This as-of-yet unexploited strategy for BVMO engineering may prove to be valuable in BVMO biocatalyst development.

$CHMO_{Loose}$ and $CHMO_{Tight}$ Are Consistent with the BVMO Structural Mechanism. With the report of the $CHMO_{Rotated}$ crystal structure,[28] it was possible to propose a complete structural mechanism for the BVMOs (see Figure S1). This mechanism was able to rationalize both the broad substrate specificity and high stereospecificity of CHMO[23] while keeping NADP(H) bound throughout the catalytic cycle. In doing so, a three-state substrate binding mechanism was suggested, involving two substrate/product-associated states that had yet to be observed. Combining the new $CHMO_{Tight}$ and $CHMO_{Loose}$ crystal structures with the previously reported $CHMO_{Rotated}$ structure, we now have a crystal structure with either substrate or product bound for each of the six critical substrate- and product-bound states proposed in the BVMO structural mechanism.[28] These are also all structures of the same enzyme, allowing them to be compared directly. The $CHMO_{Rotated}$ crystal structure corresponds to the Criegee-like states (*states F and G*), which are characterized by a closed off binding pocket that is large enough to accommodate a wide range of larger substrates. The $CHMO_{Tight}$ structure corresponds to the states just prior to and just following the Criegee-like states (*states E and H*), which are characterized by a more specific Tight-binding pocket that is not solvent exposed. Finally, the $CHMO_{Loose}$ structure corresponds to the states just prior to and just following the Tight-binding states (*states D and I*), which allow a Loose association between the enzyme and the substrate or product by virtue of the fact that the loop is disordered, the NADPH-binding domain is rotated away from the active site, and the binding pocket is solvent exposed. This third structure is the only one of the three that has the substrate or product completely solvent exposed and able to associate or dissociate easily with the enzyme.

Conclusion. The $CHMO_{Loose}$ and $CHMO_{Tight}$ crystal structures provide the first examples of crystal structures of BVMOs with a true substrate or product bound in the position initially predicted based on the $CHMO_{Closed}$ structure. Given that these structures place the product in close proximity to

those residues important for the enzyme's stereospecificity, they provide for the first time a structural framework for the stereospecificity of the enzyme. Based on this framework, we are able to rationalize the stereospecificity of two BVMOs and one mutant with regard to five different substrates. While structures involving large or asymmetric substrates or products are still needed to fully understand the substrate profile and stereospecificity of the BVMOs, these structures provide an important foundation for future protein design studies. It should be noted that this stereochemical framework is consistent with the structural catalytic mechanism that we previously proposed.[28]

In addition, the role of protein dynamics in the complex catalytic cycle is re-emphasized. The domain rotations that have been observed when comparing previous crystal structures are highlighted again when these two new structures are added. In addition, the role of the large loop can be expanded. There is increased evidence that the loop undergoes multiple order−disorder transitions per catalytic cycle. In addition, we have shown for the first time that a key loop mutant is able to affect the enzyme's substrate profile and stereospecificity, highlighting another possible avenue for protein engineering.

METHODS

For a description of the creation of the W492A mutant, the substrate profiling studies, and the modeling of substituted substrates for determination of enzyme directionality, please consult the Supporting Information.

Purification and Crystallization. *Rm*CHMO was purified as previously described,[28] except that the HiLoad Superdex 75 26/60 prep grade column was equilibrated and the sample eluted with 50 mM Tris buffer, pH 8.0. The protein was then concentrated to 5−8 mg mL^{-1} and supplemented with a 5-fold molar excess of FAD and $NADP^+$. Crystals were obtained using the sitting drop vapor diffusion method in MRC2 crystallization plates. In brief, 2 μL of the protein sample were mixed with 1 μL of reservoir solution over an 85 μL reservoir of 100 mM bicine or imidazole buffer, pH 8.0, 45−60% (w/v) PEG 3350, and 0.1−0.25 M ϵ-caprolactone. The plate was incubated at 4 °C, and crystals were obtained within 1 week.

For the cross-linking studies, the method of Lusty[34] was used. A 4 μL drop consisting of 100 mM imidazole pH 8.0, 50% (w/v) PEG 3350, and 0.2 M ϵ-caprolactone was placed on an 18 mm siliconized coverslip (Hampton Research) and suspended over a 1 mL reservoir containing the same solution in a 24-well ComboPlate (Greiner Bio-One). Crystals were transferred from the mother liquor to this new drop for cross-linking. This is to avoid reactivity with the primary amine of Tris. A microliter of concentrated hydrochloric acid was added to 1 mL of a 25% aqueous solution of glutaraldehyde obtained from Sigma-Aldrich (G5882). A 2 μL drop of this solution was added to the coverslip without allowing it to mix with the drop containing crystals. The plate was incubated at room temperature for 30 min, and then at 4 °C for 30 min, after which the glutaraldehyde drop was removed. The plate was allowed to stand overnight at 4 °C, after which 1 μL of 1 M ϵ-caprolactone was added to the crystal drop. The plate was incubated at 4 °C overnight.

Data Collection and Structure Solution. Data were collected under standard cryogenic conditions. For the $CHMO_{Tight}$ crystal, data were collected at beamline 08ID-1 at the Canadian Light Source. For the $CHMO_{Loose}$ crystal, data were collected on a Rigaku MicroMax-007HF generator equipped with VariMax HF optics and a Saturn 944+ CCD detector. The data were processed using the HKL2000 suite of programs (Table 1).[35] The $CHMO_{Rotated}$ structure and the $CHMO_{Tight}$ structure, with ligands removed, were used as the starting models for the refinement of the $CHMO_{Tight}$ and $CHMO_{Loose}$ structures, respectively. The models were subjected to multiple rounds of positional and B-factor refinement using Refmac.[36] Manual model building was performed regularly during refinement using Coot.[37]

Table 1. Data Collection and Refinement Statistics for the $CHMO_{Tight}$ and $CHMO_{Loose}$ Crystal Structures

	$CHMO_{Tight}$ (PDB ID 4RG3)	$CHMO_{Loose}$ (PDB ID 4RG4)
data collection statistics		
space group	$P2_12_12_1$	$P2_12_12_1$
a, *b*, *c* (Å)	55.7, 67.1, 131.6	55.1, 67.0, 133.6
resolution range (Å)	24.03−1.94	42.6−2.5
completeness (%)[a]	98.3 (91.4)	94.4 (77.5)
redundancy[a]	13.4 (12.7)	3.7 (1.7)
reflections with $I/\sigma<2$ (%)[a]	19.6 (53.2)	27.6 (43.8)
refinement statistics		
total number of reflections (reflections in R_{free} set)	36,235 (3670)	16,591 (1678)
R_{factor} (%) (work + free/free)	17.0/21.8	19.1/26.4
number of atoms	4323	4044
-protein	4065	3872
-water	138	53
-cofactors and product	109	109
-other	11	10
RMSD		
-bond length (Å)	0.017	0.014
-bond angle (deg)	1.829	1.795
Ramachandran plot	526 (100%)	505 (100%)
-residues in favored positions	504 (95.82%)	475 (94.06%)
-residues in allowed positions	21 (3.99%)	26 (5.15%)
-residues in disallowed positions	1 (0.19%)	4 (0.79%)

[a]Numbers in parentheses refer to the highest resolution shell.

Coordinates and structure factors were deposited to the PDB as PDB ID 4RG3 ($CHMO_{Tight}$) and PDB ID 4RG4 ($CHMO_{Loose}$). Structural figures were prepared using PyMOL (Schrödinger LLC).

ASSOCIATED CONTENT

Supporting Information

Creation of the W492A mutant, substrate profiling of the wild-type and W492A mutant, rotation of the NADPH-binding domain in the five CHMO structures, comparison of the $CHMO_{Tight}$ and $CHMO_{Loose}$ active site regions, assessment of the directionality of the BVMOs based on terpenone regiospecificity, and large substrate Criegee intermediate models based on the $CHMO_{Tight}$ and $CHMO_{Rotated}$ crystal structures. This material is available free of charge via the Internet at http://pubs.acs.org.

Accession Codes

$CHMO_{Tight}$: PDB ID 4RG3. $CHMO_{Loose}$: PDB ID 4RG4.

AUTHOR INFORMATION

Corresponding Author

*E-mail: albert.berghuis@mcgill.ca.

Notes

The authors declare no competing financial interest.

ACKNOWLEDGMENTS

The authors would like to thank all of the past and present members of the Berghuis lab for all of their assistance and suggestions. The data for the $CHMO_{Tight}$ crystal structure were collected at the Canadian Light Source beamline 08ID-1 by Shaun Labiuk; we would like to thank him for his assistance. The research presented here was made possible through grants from the Natural Sciences and Engineering Research Council of

Canada (NSERC RGPIN 183867-13) and the Canadian Institute of Health Research (CIHR MOP-114889) awarded to A.M.B. B.J.Y. has held scholarships from the Natural Sciences and Engineering Research Council of Canada, McGill University, the CIHR Strategic Initiative in Chemical Biology, and the NSERC CREATE Program in Bionanomachines. A.M.B. holds a Canada Research Chair in Structural Biology. P.C.K.L. would like to thank the Fonds québécois de la recherche sur la nature et les technologies Center for Green Chemistry and Catalysis for partial support.

REFERENCES

(1) Baeyer, A., and Villiger, V. (1899) Einwirkung des Caro'schen Reagens auf Ketone. *Ber. Dtsch. Chem. Ges. 32*, 3625−3633.
(2) Baeyer, A., and Villiger, V. (1900) Ueber die Einwirkung des Caro'schen Reagens auf Ketone. *Ber. Dtsch. Chem. Ges. 33*, 858−864.
(3) Krow, G. R. (1993) The Baeyer−Villiger Oxidation of Ketones and Aldehydes, in *Organic Reactions* (Paquette, L. A., Ed.), pp 251−798, John Wiley & Sons, Inc., New York, NY.
(4) Strukul, G. (1998) Transition Metal Catalysis in the Baeyer-Villiger Oxidation of Ketones. *Angew. Chem., Int. Ed. 37*, 1198−1209.
(5) ten Brink, G. J., Arends, I. W. C. E., and Sheldon, R. A. (2004) The Baeyer−Villiger Reaction: New Developments toward Greener Procedures. *Chem. Rev. 104*, 4105−4124.
(6) Donoghue, N. A., and Trudgill, P. W. (1975) The Metabolism of Cyclohexanol by *Acinetobacter* NCIB 9871. *Eur. J. Biochem. 60*, 1−7.
(7) Donoghue, N. A., Norris, D. B., and Trudgill, P. W. (1976) The Purification and Properties of Cyclohexanone Oxygenase from *Nocardia globerula* CL1 and *Acinetobacter* NCIB 9871. *Eur. J. Biochem. 63*, 175−192.
(8) Kayser, M. M. (2009) 'Designer reagents' recombinant microorganisms: new and powerful tools for organic synthesis. *Tetrahedron 65*, 947−974.
(9) Alphand, V., and Wohlgemuth, R. (2010) Applications of Baeyer-Villiger Monooxygenases in Organic Synthesis. *Curr. Org. Chem. 14*, 1928−1965.
(10) de Gonzalo, G., Mihovilovic, M. D., and Fraaije, M. W. (2010) Recent Developments in the Application of Baeyer-Villiger Monooxygenases as Biocatalysts. *ChemBioChem. 11*, 2208−2231.
(11) Lau, P. C. K., Leisch, H., Yachnin, B. J., Mirza, I. A., Berghuis, A. M., Iwaki, H., and Hasegawa, Y. (2010) Sustained Development in Baeyer-Villiger Biooxidation Technology, in *Green Polymer Chemistry: Biocatalysis and Biomaterials* (Cheng, H. N., and Gross, R. A., Eds.), pp 343−372, American Chemical Society, Washington, DC.
(12) Torres Pazmiño, D. E., Dudek, H. M., and Fraaije, M. W. (2010) Baeyer-Villiger monooxygenases: recent advances and future challenges. *Curr. Opin. Chem. Biol. 14*, 138−144.
(13) Leisch, H., Morley, K., and Lau, P. C. K. (2011) Baeyer−Villiger Monooxygenases: More Than Just Green Chemistry. *Chem. Rev. 111*, 4165−4222.
(14) Reetz, M. T., Brunner, B., Schneider, T., Schulz, F., Clouthier, C. M., and Kayser, M. M. (2004) Directed Evolution as a Method To Create Enantioselective Cyclohexanone Monooxygenases for Catalysis in Baeyer−Villiger Reactions. *Angew. Chem., Int. Ed. 43*, 4075−4078.
(15) Bocola, M., Schulz, F., Leca, F., Vogel, A., Fraaije, M. W., and Reetz, M. T. (2005) Converting Phenylacetone Monooxygenase into Phenylcyclohexanone Monooxygenase by Rational Design: Towards Practical Baeyer-Villiger Monooxygenases. *Adv. Synth. Catal. 347*, 979−986.
(16) Kayser, M. M., and Clouthier, C. M. (2006) New Bioorganic Reagents: Evolved Cyclohexanone Monooxygenase—Why Is It More Selective? *J. Org. Chem. 71*, 8424−8430.
(17) Mihovilovic, M. D., Rudroff, F., Winninger, A., Schneider, T., Schulz, F., and Reetz, M. T. (2006) Microbial Baeyer-Villiger Oxidation: Stereopreference and Substrate Acceptance of Cyclohexanone Monooxygenase Mutants Prepared by Directed Evolution. *Org. Lett. 8*, 1221−1224.
(18) Torres Pazmiño, D. E., Snajdrova, R., Rial, D. V., Mihovilovic, M. D., and Fraaije, M. W. (2007) Altering the Substrate Specificity and Enantioselectivity of Phenylacetone Monooxygenase by Structure-Inspired Enzyme Redesign. *Adv. Synth. Catal. 349*, 1361−1368.
(19) Reetz, M. T., and Wu, S. (2008) Greatly reduced amino acid alphabets in directed evolution: making the right choice for saturation mutagenesis at homologous enzyme positions. *Chem. Commun. (Camb.)*, 5499−5501.
(20) Reetz, M. T., and Wu, S. (2009) Laboratory Evolution of Robust and Enantioselective Baeyer−Villiger Monooxygenases for Asymmetric Catalysis. *J. Am. Chem. Soc. 131*, 15424−15432.
(21) Dudek, H. M., de Gonzalo, G., Torres Pazmiño, D. E., Stepniak, P., Wyrwicz, L. S., Rychlewski, L., and Fraaije, M. W. (2011) Mapping the Substrate Binding Site of Phenylacetone Monooxygenase from *Thermobifida fusca* by Mutational Analysis. *Appl. Environ. Microbiol. 77*, 5730−5738.
(22) Malito, E., Alfieri, A., Fraaije, M. W., and Mattevi, A. (2004) Crystal structure of a Baeyer-Villiger monooxygenase. *Proc. Natl. Acad. Sci. U. S. A. 101*, 13157−13162.
(23) Mirza, I. A., Yachnin, B. J., Wang, S., Grosse, S., Bergeron, H., Imura, A., Iwaki, H., Hasegawa, Y., Lau, P. C. K., and Berghuis, A. M. (2009) Crystal Structures of Cyclohexanone Monooxygenase Reveal Complex Domain Movements and a Sliding Cofactor. *J. Am. Chem. Soc. 131*, 8848−8854.
(24) Orru, R., Dudek, H. M., Martinoli, C., Torres Pazmiño, D. E., Royant, A., Weik, M., Fraaije, M. W., and Mattevi, A. (2011) Snapshots of Enzymatic Baeyer-Villiger Catalysis. *J. Biol. Chem. 286*, 29284−29291.
(25) Leisch, H., Shi, R., Grosse, S., Morley, K., Bergeron, H., Cygler, M., Iwaki, H., Hasegawa, Y., and Lau, P. C. K. (2012) Cloning, Baeyer-Villiger Biooxidations, and Structures of the Camphor Pathway 2-Oxo-Δ^3-4,5,5-Trimethylcyclopentenylacetyl-Coenzyme A Monooxygenase of *Pseudomonas putida* ATCC 17453. *Appl. Environ. Microbiol. 78*, 2200−2212.
(26) Bosserman, M. A., Downey, T., Noinaj, N., Buchanan, S. K., and Rohr, J. (2013) Molecular Insight into Substrate Recognition and Catalysis of Baeyer-Villiger Monooxygenase MtmOIV, the Key Frame-Modifying Enzyme in the Biosynthesis of Anticancer Agent Mithramycin. *ACS Chem. Biol. 8*, 2466−2477.
(27) Beam, M. P., Bosserman, M. A., Noinaj, N., Wehenkel, M., and Rohr, J. (2009) Crystal Structure of Baeyer−Villiger Monooxygenase MtmOIV, the Key Enzyme of the Mithramycin Biosynthetic Pathway. *Biochemistry 48*, 4476−4487.
(28) Yachnin, B. J., Sprules, T., McEvoy, M. B., Lau, P. C. K., and Berghuis, A. M. (2012) The Substrate-Bound Crystal Structure of a Baeyer−Villiger Monooxygenase Exhibits a Criegee-like Conformation. *J. Am. Chem. Soc. 134*, 7788−7795.
(29) Bermúdez, E., Ventura, O. N., Eriksson, L. A., and Saenz-Méndez, P. (2014) Improved homology model of cyclohexanone monooxygenase from *Acinetobacter calcoaceticus* based on multiple templates. *Comput. Biol. Chem. 49*, 14−22.
(30) Polyak, I., Reetz, M. T., and Thiel, W. (2012) Quantum Mechanical/Molecular Mechanical Study on the Mechanism of the Enzymatic Baeyer−Villiger Reaction. *J. Am. Chem. Soc. 134*, 2732−2741.
(31) Polyak, I., Reetz, M. T., and Thiel, W. (2013) Quantum mechanical/molecular mechanical study on the enantioselectivity of the enzymatic baeyer-villiger reaction of 4-hydroxycyclohexanone. *J. Phys. Chem. B 117*, 4993−5001.
(32) Salem, M., Mauguen, Y., and Prangé, T. (2010) Revisiting glutaraldehyde cross-linking: the case of the Arg-Lys intermolecular doublet. *Acta. Crystallogr. F F66*, 225−228.
(33) Cernuchova, P., and Mihovilovic, M. D. (2007) Microbial Baeyer-Villiger oxidation of terpenones by recombinant whole-cell biocatalysts-formation of enantiocomplementary regioisomeric lactones. *Org. Biomol. Chem. 5*, 1715−1719.
(34) Lusty, C. J. (1999) A gentle vapor-diffusion technique for cross-linking of protein crystals for cryocrystallography. *J. Appl. Crystallogr. 32*, 106−112.

(35) Otwinowski, Z., and Minor, W. (1997) Processing of X-ray diffraction data collected in oscillation mode, in *Methods Enzymol.*, pp 307−326, Academic Press, Waltham, MA.
(36) Murshudov, G. N., Vagin, A. A., and Dodson, E. J. (1997) Refinement of Macromolecular Structures by the Maximum-Likelihood Method. *Acta Crystallogr. D D53*, 240−255.
(37) Emsley, P., Lohkamp, B., Scott, W. G., and Cowtan, K. (2010) Features and development of Coot. *Acta Crystallogr. D D66*, 486−501.